Inhibition of striatal dopamine release by the L-type calcium channel inhibitor isradipine co-varies with risk factors for Parkinson's

Katherine R. Brimblecombe*[1,2,4], Natalie Connor-Robson[1,2], Carole J. R. Bataille[3,4], Bradley M. Roberts[1,2], Caitlin Gracie[1], Bethan O'Connor[1], Rebecca te Water Naude[1], Gayathri Karthik[1], Angela J. Russell[3,4], Richard Wade-Martins[1,2,5], Stephanie J. Cragg[1,2,5]

Affiliations:
[1]Department of Physiology, Anatomy and Genetics, University of Oxford, OX1 3PT, UK
[2]Oxford Parkinson's Disease Centre, University of Oxford, United Kingdom
[3]Department of Chemistry, Chemistry Research Laboratory, University of Oxford, OX1 3TA
[4]Department of Pharmacology, University of Oxford, OX1 3QT
[5]Aligning Science Across Parkinson's (ASAP) Collaborative Research Network, Chevy Chase, MD 20815, USA

Running title: L-type calcium channel role in DA axons

ORCID IDs: KRB 0000-0003-0809-7292; NCR 0000-0001-8350-6928; CJRB 0000-0002-3963-0021; BMR 0000-0002-5192-2545; RtWN 0000-0002-1350-3163; GC 0000-0003-1876-0975; AJR 0000-0003-3610-9369; RWM 0000-0001-6691-580X; SJC 0000-0001-9677-2256

***Correspondence should be addressed to:**
Dr Katherine Brimblecombe
Department of Physiology, Anatomy & Genetics
University of Oxford, OX1 3PT Oxford, UK
Email: katherine.brimblecombe@dpag.ox.ac.uk

Acknowledgements
The work was funded by grant support from Parkinson's UK (J-1403; G-1803) and a Clarendon Fund/Christ Church Oxford Studentship to BMR. This research was funded in part by Aligning Science Across Parkinson's [ASAP-020370] through the Michael J. Fox Foundation for Parkinson's Research (MJFF).

Ethics statement
All procedures were licensed to be carried out at the University of Oxford under the UK Animals (Scientific Procedures) Act 1986.

Declarations of interest
The authors declare no competing interests

Data availability
Data for all figures and code is available at: 10.5281/zenodo.7801868. Step-by-step experimental protocols are available at 10.17504/protocols.io.4r3l27dxxg1y/v1

Abstract

Ca^{2+} entry into nigrostriatal dopamine (DA) neurons and axons via L-type voltage-gated Ca^{2+} channels (LTCCs) contributes respectively to pacemaker activity and DA release, and has long been thought to contribute to vulnerability to degeneration in Parkinson's disease. LTCC function is greater in DA axons and neurons from substantia nigra pars compacta than from ventral tegmental area, but this is not explained by channel expression level. We tested the hypothesis that LTCC-control of DA release is governed rather by local mechanisms, focussing on candidate biological factors known to operate differently between types of DA neurons and/or be associated with their differing vulnerability to parkinsonism, including biological sex, α-synuclein, DA transporters (DATs), and calbindin-D28k (Calb1). We detected evoked DA release *ex vivo* in mouse striatal slices using fast-scan cyclic voltammetry, and assessed LTCC support of DA release by detecting the inhibition of DA release by the LTCC inhibitors isradipine or CP8. Using genetic knockouts or pharmacological manipulations we identified that striatal LTCC support of DA release depended on multiple intersecting factors, in a regionally and sexually divergent manner. LTCC function was promoted by factors associated with Parkinsonian risk, including male sex, α-synuclein, DAT, and a dorsolateral co-ordinate, but limited by factors associated with protection i.e. female sex, glucocerebrosidase activity, Calb1, and ventromedial co-ordinate. Together, these data show that LTCC function in DA axons, and isradipine effect, are locally governed and suggest they vary in a manner that in turn might impact on, or reflect, the cellular stress that leads to parkinsonian degeneration.

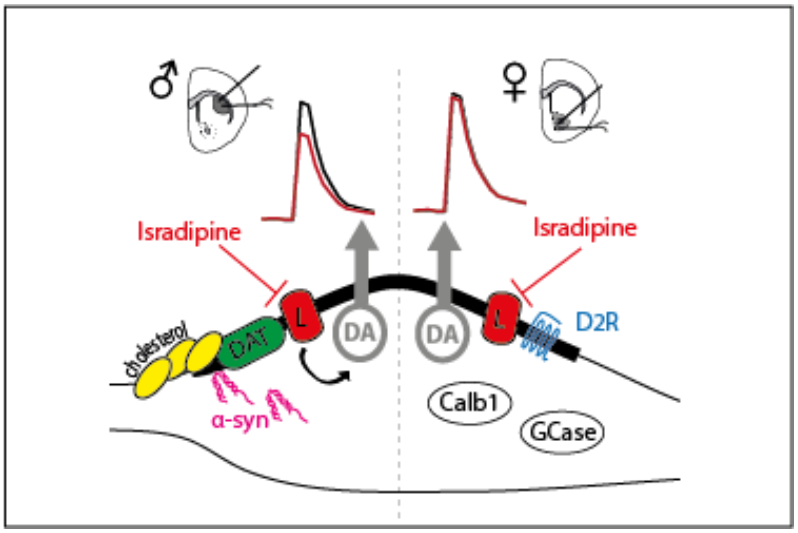

Keywords

Dopamine release; L-type calcium channel; dopamine transporter; Calb1; dopamine D2 receptor; striatum; Parkinson's disease; sex differences; synuclein

Introduction

Ca^{2+} entry via voltage-gated Ca^{2+} channels (VGCCs) is important for pacemaker activity in dopamine (DA) neurons within the substantia nigra pars compacta (SNc) and critical for release of DA in the striatum (Guzman et al., 2009; Brimblecombe et al., 2015). However, Ca^{2+} also generates metabolic stress that promotes vulnerability of SNc DA neurons to degeneration in Parkinson's disease (PD) (Surmeier et al., 2010). SNc DA neurons and their axons in dorsolateral striatum (DLS) are particularly vulnerable to parkinsonian degeneration, whereas DA neurons in ventral tegmental area (VTA) and their axons in ventral striatum (nucleus accumbens, NAc) are relatively spared. L-type VGCCs (LTCCs) support pacemaker activity, by facilitating ATP production in SNc (Zampese et al., 2022) and DA release in DLS, whereas in VTA and NAc, LTCCs do not operate strongly (Guzman et al., 2009; Brimblecombe et al., 2015; Zampese et al., 2022). However, this regional difference is not reflected by LTCC expression at the level of midbrain DA neurons where LTCC expression is greater in VTA (Poulin et al., 2014), suggesting that regulatory mechanisms locally govern function. Here, we explored factors that locally regulate the LTCC support of DA release from striatal DA axons in DLS vs NAc core.

Several biological factors and mechanisms that have direct relevance to the biology of DA neurons and/or to PD are candidates for LTCC regulators. On a population level, after aging, the biggest risk factor for PD is biological sex: men are twice as likely as women to develop PD (Wooten et al., 2004) but the biology underlying this difference is poorly understood. It has been established in cardiac myocytes that LTCC function is greater in males than females (Curl et al., 2008), but sex differences in LTCC function in central DA systems have not previously been explored. Here, we explored how LTCCs support DA release in both sexes of mice, and define sex differences.

Several genetic mutations and polymorphisms confer an increased risk to PD (Bekris et al., 2010). These range from rare, high penetrance mutations e.g. in the genes for α-synuclein (*SNCA*) and PINK-1/Parkin, to more common, less penetrant single-nucleotide polymorphisms, discovered by GWAS including *GBA* (gene encoding glucocerebrosidase, GCase) as the most commonly associated genetic risk factor. Interestingly, variants in *SNCA* occur as both rare, high penetrance and common, low penetrance forms. Here, we tested whether α-synuclein or GCase levels could impact on LTCC support of DA release.

We also tested whether several known physiological regulators of DA output from SNc and VTA DA neurons might support a differential contribution of LTCCs to DA release. We focussed on calbindin-D28K (Calb1), the DAT, and DA D_2-receptors (D_2Rs), each of which have been reported to interact with LTCCs in different systems. Calb1 is enriched in PD-resistant VTA neurons (Gerfen et al., 1987; Poulin et al., 2014), limits DA release in NAc (Brimblecombe et al., 2019) and, in cellular expression systems, can bind to and limit function of LTCCs (Lee et al., 2006). We report here that Calb1 limits LTCC support of DA

release in a regionally and sexually divergent manner. DATs are enriched in SNc and VTA DA neurons, with highest expression levels reported in SNc, in both mouse and human brains (Ciliax et al., 1995; Poulin et al., 2014), and differential DAT expression has long been hypothesised to be a driving factor in sensitivity to PD on cellular and population levels (Ritz et al., 2009; Lohr et al., 2017). In cellular expression systems, DATs and other electrogenic monoamine transporters promote LTCC currents (Cameron et al., 2015). We report here that DATs play a role in facilitating how LTCCs support axonal DA release. Lastly, D2Rs are described as more enriched in SNc than VTA DA neurons (Greene et al., 2005; Poulin et al., 2014), and can inhibit LTCC function (via βγ-inhibition) in striatal GABAergic projection neurons (Hernández-López et al., 2000; Olson et al., 2005). Despite D2Rs not being associated with either risk or protection in PD (not least due to their broad expression pattern), they are well placed to modulate LTCC support of DA release. We report here that D2Rs operate a limiting factor on LTCC function in NAc. Overall, we reveal a network of factors that, by either inhibiting or facilitating LTCC function in DA axons, contribute to a greater role for LTCCs in supporting DA release in DLS than NAc, and in males than females, and a correspondingly varying outcome of LTCC inhibitor isradipine on DA release.

Materials and methods

Animals

We used male and female adult mice aged 3-10 months. Wild-type mice were C57Bl6/J (Charles River). Calbindin-knockdown (CalbKD) animals were generated by crossing homozygous DAT$^{IRES\,cre}$ (https://www.jax.org/strain/006660) mice with homozygous Calb$_{TM2}$ mice (loxP sites flanking Exon1) (Barski et al., 2002) donated by Prof. Meyer (University of Munich) (available from Jax https://www.jax.org/strain/031936 and EMMA: strain name B6.(R1)-Calb1tm2Mpin), generating double-heterozygous offspring with decreased calb1 expression in DAT-expressing cells as previously published (Brimblecombe et al., 2019). CalbWT control mice were age- and sex-matched heterozygous DAT$^{IRES\,cre}$ mice. *SNCA*-OVX and *Snca*-null mice were generated in house as previously published (Janezic et al., 2013) (OVX https://www.jax.org/strain/023837; null https://www.jax.org/strain/003692). *Gba*$^{+/-}$ mice were purchased from Jax (https://www.jax.org/strain/002594).

Slice preparation

Mice were killed by cervical dislocation, the brains removed, and 300 µm coronal striatal slices prepared as described previously (Brimblecombe et al., 2015) in ice-cold HEPES-based buffer saturated with 95% O_2/5% CO_2, containing in mM: 120 NaCl, 20 $NaHCO_3$, 6.7 HEPES acid, 5 KCl, 3.3 HEPES salt, 2 $CaCl_2$, 2 $MgSO_4$, 1.2 KH_2PO_4, 10 glucose. Slices were incubated at room temperature for ≥ 1 hour in HEPES-based buffer before experiments. All procedures were licensed to be carried out at the University of Oxford under the UK Animals (Scientific Procedures) Act 1986.

Fast-scan cyclic voltammetry (FCV)

Ex vivo DA release was monitored in acute coronal slices using fast-scan cyclic voltammetry (FCV) as previously described (Brimblecombe et al., 2015). Slices were superfused in a recording chamber with bicarbonate-buffered artificial cerebrospinal fluid (aCSF) saturated with 95%O_2/5%CO_2 at 31–33 °C, containing in mM: 124 NaCl, 26 $NaHCO_3$, 3.8 KCl, 0.8-3.6 $CaCl_2$ (as stated), 1.3 $MgSO_4$, 1.3 KH_2PO_4, 10 glucose. Evoked extracellular DA concentration ($[DA]_o$) was monitored by FCV using a Millar voltammeter (Julian Millar, Barts and the London School of Medicine and Dentistry) and single-use carbon-fibre microelectrodes (7-10 µm diameter) fabricated in-house (tip length 50-100 µm). A triangular voltage waveform (range -700 mV to +1300 mV vs. Ag/AgCl) was applied at 800 V/s at a scan frequency of 8 Hz. Electrodes were switched out of circuit between scans. Electrodes were calibrated using 2 µM DA, prepared immediately before calibration using stock solution (2.5 mM in 0.1M $HClO_4$ stored at 4 °C). Signals were attributed to DA due to the potentials of their characteristic oxidation (500-600 mV) and reduction (-200 mV) peaks. Step-by-step methods can be found at protocols.io: 10.17504/protocols.io.4r3l27dxxg1y/v1

Electrical stimulation

DA recordings were obtained from dorsolateral quadrant of dorsal striatum, the dorsolateral striatum (DLS), or nucleus accumbens core (NAc). DA release was evoked by a local bipolar concentric Pt/Ir electrode (25 µm diameter; FHC inc. ME, USA) placed approximately 100 µm from the recording electrode. Stimulus pulses (200 µs duration) were given at 0.6 mA (perimaximal in drug-free control conditions). Stimulations were single pulses (1p) were repeated at 2.5 minute intervals. A stable pre-drug baseline of 6 stimulations before isradipine or CP8 was washed on for 12 stimulations. A stable baseline was determined during the experiment when the average peak oxidation for stimulus 5,6 was 95-105% of stimulus 1 and 2. All data were obtained in the presence of the nAChR antagonist, dihydro-β-erythroidine (DHβE, 1 µM) to exclude the strong effects of nAChRs on DA release (Zhou et al., 2001; Rice and Cragg, 2004; Cachope et al., 2012; Threlfell et al., 2012).

Drugs and solutions

Reagents were purchased from Torcis or Sigma Aldrich (cocaine, water-soluble cholesterol). Stock solutions were made to 1000-2000x final concentrations in H_2O (DHβE, cocaine), DMSO (isradipine, L-741,626, CP8), 0.1 M HCl (nomifensine) or ethanol (lidocaine) and stored at -20°C. Drugs were diluted to their required concentrations in aCSF immediately prior to use. Drug concentrations were chosen in accordance with previous studies (Acevedo-Rodriguez et al., 2014; Brimblecombe et al., 2015). Water soluble cholesterol or vehicle control Me-ß-cyclodextrin were dissolved in 10 ml aCSF, and slices were incubated and oxygenated for 30 mins before transferring to recording chamber as previously described (Threlfell et al., 2021).

CP8 synthesis

According to the method (Kang et al., 2013) 2-(3-chlorophenyl)ethylamine (357 µL, 2.58 mmol, 1.0 eq.) was added in one portion to a solution of cyclopentane isocyanate (290 mg, 2.58 mmol, 1.0 eq.) in CH_2Cl_2 (10 mL) and the reaction was stirred at room temperature for 5 h (completion was monitored by LRMS). Malonyl chloride (276 µL, 2.84 mmol, 1.1 eq.) was then added dropwise under vigorous stirring over 5 min. The resulting mixture was stirred for 1 h and concentrated *in vacuo*. The residue was purified by column chromatography on silica gel (EtOAc/pentane, 1:4) to afford the title product as a white solid (687 mg, 80%). ^{1}H NMR (400 MHz, $CDCl_3$) δ 7.25 – 7.19 (m, 3H), 7.13 (dt, *J* = 6.7, 2.1 Hz, 1H), 5.20 – 5.07 (m, 1H), 4.13 – 4.03 (m, 2H), 3.62 (s, 2H), 2.92 – 2.84 (m, 2H), 1.94 (tqd, *J* = 8.0, 4.9, 2.0 Hz, 4H), 1.89 – 1.79 (m, 2H), 1.61 – 1.57 (m, 2H); ^{13}C NMR (101 MHz, $CDCl_3$) δ 164.9, 164.6, 151.1, 140.0, 134.5, 123.0, 129.2, 127.3, 127.1, 54.6, 42.8, 40.3, 33.8, 28.8, 25.7; LRMS m/z (ESI^-) 333.1 $[M-H]^-$. The data were in accordance with those reported in the literature (Kang et al., 2013)

Data and statistical analysis

FCV data were acquired and analysed using Axoscope 10.5 (Molecular devices) and Excel macros written locally. Data are expressed as mean ± standard error of the mean (SEM), and N = number of slices (typically 1 per animal) from at least 3 animals. Data from each slice were obtained by averaging 4 recordings prior to drug wash-on (control) vs. average of 4 recordings after 20 minutes. Typically data are shown normalised to control conditions to standardise for variation in initial evoked extracellular DA concentrations ($[DA]_o$). Population means were compared using one- or two-way ANOVA with Dunnett's post-test and unpaired t-test where appropriate using GraphPad Prism (9.3.1). Curve fits were performed in GraphPad Prism. Data for all figures are available 10.5281/zenodo.7801868.

Classification tree

A classification tree was performed in R(4.2.1) (10.5281/zenodo.7801868). The normalised effect of isradipine for each individual experiment was annotated with the experimental condition: sex and genotype of mouse and presence of drug prior to washing on isradipine (fig5 data tab in xlsx file 10.5281/zenodo.7801868). These data were sorted using a classification tree using Gini impurity algorithm with a cut off of 0.91 normalised effect of isradipine, which corresponds to 2 s.d. above the mean effect of isradipine in DLS of male WT mouse (i.e. the original recording conditions where we identify a significant effect of isradipine on decreasing DA (Brimblecombe et al., 2015). It should be noted that 0.91 is also 2 s.d. below mean normalised effect of isradipine in male WT NAc (2.4 mM $[Ca^{2+}]_o$), which was our original recording conditions when we did not identify an effect of isradipine). Due to the structure of the classification tree whereby, factors were effectively sorted with no outliers (i.e. the leaves (final nodes) were mostly pure with probabilities of 0 or 1), we determined it was unsuitable to run a logistic regression analysis on these data.

160 ## Western blots

161 Mice were culled by cervical dislocation, brains extracted and dissected on ice. The striatum and midbrain
162 were extracted from both hemispheres and snap frozen. Samples were prepared for western blot as
163 previously described (Connor-Robson et al., 2019). Briefly, tissue was homogenised on ice in RIPA buffer
164 containing protease inhibitors (Roche) and protein concentration determined by BCA assay. Following
165 dilution Laemmli buffer was added and samples were boiled for 5 minutes at 95°C. Samples were loaded
166 and run on 4-15% criterion-TGX gels and transferred to PDVF membranes (BioRad). Membranes were
167 blocked for 1 hour at room temperature and then probed with primary antibody (calb1: 1:1000 Cell
168 Signalling #13176) overnight at 4°C. After incubation with HRP conjugated secondary antibodies the blot
169 was developed using chemiluminescent HRP substrate.

170 # Results

171 **Sex difference in the LTCC support of DA release**

172 We and others, have to date principally explored LTCC function in males rather than females (Guzman et
173 al., 2009, 2018; Ilijic et al., 2011; Brimblecombe et al., 2015). There is a ~2:1 prevalence of PD in males
174 and females and it is therefore important to understand the biology of LTCCs in both sexes, in order to
175 gain a fuller understanding of disease aetiology but also drug action. Here, we tested whether LTCCs
176 support DA release in DLS of female mice, which they do in male mice (Brimblecombe et al., 2015). We
177 first assessed DA release and uptake parameters. We found no difference in peak evoked extracellular
178 concentrations of DA ($[DA]_o$) evoked by single electrical stimulus pulses (1p) (**Figure 1A,B,** t-test t_{14}=0.14
179 *P=0.89*), but did find faster DA clearance rates in females (**Figure 1A,C,** T-test with Welch's correction
180 $t_{29.9}$=6.59 *P<0.0001*), consistent with greater DAT levels in the striatum of female mice (Costa et al., 2021).
181 We then tested the effect of LTCC inhibitor isradipine (5 µM) on 1p-evoked $[DA]_o$ in DLS and confirmed a
182 decrease in evoked $[DA]_o$ in male mice (**Figure 1D,** comparison of normalised peak $[DA]_o$, One-sample t-
183 test t_2=5.6, *P*=0.03, N=3) as published previously (Brimblecombe et al., 2015) but, by contrast, not in
184 female mice (**Figure 1D,** comparison of normalised peak $[DA]_o$, One-sample t-test t_4=0.87, *P*=0.44, N=5),
185 revealing a statistically significant difference between the two sexes (**Figure 1E,** Two-way ANOVA: sex x
186 drug interaction, $F_{16,67}$=3.0, *P*<0.001; main effect of sex, $F_{1,67}$=44.9, *P*<0.001).

187 **Genetic contributors to PD promote LTCC support of DA release**

188 Mutations in the *SNCA* gene including common, lower penetrance SNPs identified by GWAS (Alegre-
189 Abarrategui et al., 2019) are associated with rare monogenic forms of PD, while mutations in *GBA* are the
190 most common genetic factor in PD. We tested whether α-synuclein facilitates LTCC support of DA release,
191 using a BAC transgenic mouse line that overexpresses human wild-type α-synuclein (*SNCA*-OVX) (Janezic
192 et al., 2013), versus the background control line that are null for mouse α-synuclein (*Snca*-null). Mean

193 peak $[DA]_o$ evoked by 1p in DLS of *SNCA*-OVX mice were ~30% less than *Snca*-null mice (**Figure 1F,**
194 unpaired t-testt_{14}=2.55 *P*= 0.023) as seen previously (Janezic et al., 2013; Roberts et al., 2020; Threlfell et
195 al., 2021). In DLS of male *SNCA*-OVX mice, isradipine decreased 1p-evoked $[DA]_o$ by ~30%, (**Figure 1G,**
196 comparison of peak $[DA]_o$ t_3=6.6 *P*=0.007 N=4) as seen in WT (**Figure 1C**) (Brimblecombe et al., 2015)).
197 However, in male *Snca*-null mice, isradipine had no effect on 1p-evoked $[DA]_o$ (**Figure IG,** comparison of
198 normalised peak $[DA]_o$ t_3=0.25 *P*=0.82 N=4), showing a statistically significant difference between the two
199 genotypes (**Figure 1H,** two-way ANVOA: genotype X drug interaction, $F_{17,102}$=3.0, *P*=0.0003; main effect
200 of genotype, $F_{1,6}$=4.89 *P*=0.002) and suggesting a dependence of LTCC function on α-synuclein.

201 We did not see an LTCC role in DA release in females in WT mice (see Figure 1C), but tested
202 whether LTCC support of DA release in females could be established in either of two different PD-related
203 mouse lines. Firstly, we explored whether overexpression of α-synuclein could result in LTCC support of
204 DA release. However, in female *SNCA*-OVX mice, isradipine did not decrease $[DA]_o$ in DLS (**Figure 1I,**
205 comparison of normalised peak $[DA]_o$ t_2=2.2 *P*=0.16), indicating a significant difference between male and
206 female *SNCA*-OVX mice (**Figure 1J,** two-way ANVOA: genotype X drug interaction, $F_{17,102}$=1.89, *P*=0.027;
207 main effect of genotype, $F_{1,6}$=7.85 *P*=0.03). Secondly, since mutations in the GCase *GBA* gene are
208 associated with PD and seen more commonly in women with PD than men (Li et al., 2021) we explored
209 whether LTCC support of DA release varied with GCase levels in females, by comparing mice that were
210 heterozygous for the mouse *Gba* gene *(Gba*$^{+/-}$) with wild-type littermate homozygous controls (*Gba*$^{+/+}$).
211 Isradipine did not modify 1p-evoked $[DA]_o$ in DLS *Gba*$^{+/+}$ female controls, as seen for other wild-type
212 females, but strikingly, isradipine did inhibit 1p-evoked $[DA]_o$ in female *Gba*$^{+/-}$ mice (**Figure 2K,**
213 comparison of normalised peak $[DA]_o$, *Gba*$^{+/+}$(WT), t_2=0.33 *P*=0.77; *Gba*$^{+/-}$, t_4=12.03 *P*=0.0003), showing a
214 significant difference between these two genotypes (**Figure 1L:** two-way ANVOA: genotype X drug
215 interaction $F_{16,96}$=6.4 *P*<0.0001; main effect of genotype, $F_{1,6}$=16.2 *P*=0.007). These observations indicate
216 that a role for LTCCs in supporting DA release is exposed when GCase function is compromised.

217 We note that across all experiments and variables, we found no correlation between 1p-evoked
218 $[DA]_o$ levels and the subsequent effect of isradipine (**Figure 1M,** simple linear regression, slope does not
219 significantly differ from zero $F_{1,28}$=0.049 *P* = 0.83) confirming that effect size was not a function of
220 different initial release probability in different conditions.

221 **Sex differences and calb1 interact to govern LTCC function**

222 VTA and SNc DA neurons differ in a number of key aspects that might contribute to their differing
223 sensitivities to parkinsonian degeneration. One notable difference is the greater expression of calbindin-
224 D28K (Calb1) in VTA neurons, which has been suspected to be protective against PD, although evidence
225 is mixed (Airaksinen et al., 1997; Yuan et al., 2013). We used cre-lox P recombination to selectively
226 knockdown Calb1 in DA neurons in a cross of DAT-Cre mice with floxed Calb1 mice as previously

227 (Brimblecombe et al., 2019) which does not affect evoked $[DA]_o$ or DA uptake in DLS, but it has profound
228 impact in NAc, consistent with the regional endogenous expression profile of Calb1. We found here that
229 in control mice (DAT-Cre hets, referred to as CalbWT), isradipine decreased 1p-evoked $[DA]_o$ in males in
230 DLS but not NAc, and did not modify evoked $[DA]_o$ in females in DLS (**Figure 2A**) as per wild-type mice
231 (see Fig 1). By contrast, in CalbKD mice, isradipine decreased 1p-evoked $[DA]_o$ in male DLS and NAc, and
232 in female DLS (**Figure 2B**). Overall, Calb1 knockdown significantly increased the effect of isradipine on
233 DA release (**Figure 2C,** 2-way ANOVA effect of genotype $F_{1,14}$=31.17 *P<0.001*) and enabled LTCCs to
234 support DA release in both male NAc and female DLS. We tested whether there was a gross upregulation
235 of Calb1 levels in the striatum of wild-type female mice relative to males, leading to the occlusion of LTCC
236 function seen in WT female mice. However western blot analysis of protein levels in whole striatal tissue
237 did not detect a difference in Calb1 expression in striatum of females vs males (**Fig 2D,E,** unpaired t-test
238 T_4=0.18 *P*=0.86).

239 **DAT function promotes LTCC support of DA release**

240 Translocation of DA across the membrane by DAT involves the co-transport of 2 Na^+ and 1 Cl^-, an
241 electrogenic process that can depolarise DA neuron membranes, independently of DA translocation
242 (Ingram et al., 2002) and in cellular expression systems can activate LTCCs (Cameron et al., 2015). We
243 tested whether DATs operate in DA axons to support LTCC function. We inhibited DATs using cocaine (5
244 µM) or nomifensine (10 µM), monoamine uptake inhibitors which are also known to prevent the
245 electrogenic effects of DAT (Sonders et al., 1997), and tested the impact of isradipine on 1p-evoked $[DA]_o$
246 in DLS in male wild-type mice. We found that in the presence of cocaine or nomifensine, the effect of
247 LTCC inhibitor isradipine in the DLS was no longer apparent (**Figure 3A-C,** Two-way ANOVA: isradipine x
248 pre-condition interaction $F_{32,192}$=3.57, P<0.001; comparison of peaks 1-sample t-test: control t_3=6.48,
249 P=0.0074, cocaine t_4=0.37 *P* = 0.73, nomifensine t_4=1.39 *P*=0.23). The loss of isradipine effect in the
250 presence of cocaine was not due to any potential effects of cocaine as an inhibitor of voltage-gated Na^+-
251 channels (Na_v) because application of the Na_v blocker and analogue lidocaine did not similarly prevent
252 the effect of isradipine. Rather, in the presence of lidocaine, isradipine decreased 1p-evoked $[DA]_o$ as
253 seen in standard conditions (**Figure 3C,** 1-way ANOVA $F_{2,9}$=11.5 *P* = 0.03, Dunnett's post-test lidocaine vs
254 control *P*= 0.83, cocaine vs control *P* = 0.003, nomifensine vs control *P*= 0.014). These data show that
255 inhibition of DATs occludes LTCCs from contributing to DA release and suggest that DATs support LTCC
256 function in DLS.

257 We tested whether a potentiation of DAT function could facilitate LTCC support of DA release
258 where it was not previously observable. We have previously shown that DAT function in *Snca*-null mice
259 can be augmented by cholesterol (Threlfell et al., 2021) and exploited this action to see whether in *Snca*-
260 null male mice an effect of isradipine could be brought about after cholesterol incubation and its allied

261 increase in DAT function. Indeed, after incubation in cholesterol, isradipine significantly decreased 1p-
262 evoked $[DA]_o$ (**Figure 3D,** control: t_3=4.2 *P*=0.025). To confirm that this outcome depended on DAT
263 function, we repeated in the presence of cocaine to inhibit DAT. In the presence of cocaine, cholesterol
264 incubation no longer supported an effect of isradipine on DA release (**Figure 3D,** cocaine: t_3=0.17 *P*=0.87,
265 **Figure 3E,** one-way ANOVA $F_{3,12}$=6.29 *P*= 0.0083, Dunnett's post-test *Snca*-null control vs cholesterol
266 *P*=0.0034, vs chol+cocaine *P*=0.54), suggesting that a DAT-dependent increase in LTCC function underlay
267 this impact of cholesterol.

268 We excluded an alternative hypothesis that DAT function promotes the effect of isradipine not
269 by increasing LTCC function but by changing the ability of isradipine to bind to LTCCs. It is known that at
270 hyperpolarised potentials, isradipine does not effectively bind to LTCC (Helton et al., 2005; Rey et al.,
271 2020). Since inhibitors of DATs will reduce DAT-associated depolarising electrogenic currents and
272 maintain DA axons in a more hyperpolarised state, they might prevent isradipine from binding to LTCC.
273 We therefore tested whether the actions of an alternative LTCC antagonist to isradipine, CP8, which binds
274 LTCCs in a voltage-independent manner (Kang et al., 2013; Rey et al., 2020), were also prevented in the
275 presence of cocaine. We found firstly that CP8 decreased 1p-evoked $[DA]_o$ in DLS of male mice, but not
276 in male NAc (**Figure 3F,G,** t-test comparison on peak DLS: t_2=5.19 *P*=0.035, DLS+cocaine t_3=1.39 *P*=0.26,
277 NAc: t_2=1.54 *P*=0.26; Two-way ANOVA post-test time point 10 vs 40 min DLS: *P* = 0.0052. NAc (not shown):
278 *P* = 0.78, DLS+cocaine *P* = 0.99), paralleling the effects of isradipine. Further in parallel with the effects of
279 isradipine, CP8 did not reduce 1p-evoked $[DA]_o$ in DLS in the presence of cocaine (**Figure 3G,** 2-way
280 ANOVA post-test time point 10 vs 40 min DLS: *P* = 0.0052. NAc: *P* = 0.78, DLS+cocaine *P* = 0.99). These
281 data indicate that DATs indeed support LTCC function in contributing to DA release and do not simply
282 support the voltage-sensitive binding and action of isradipine.

283 **D2Rs limit LTCC function in NAc**

284 We tested whether D2R activity modifies how LTCCs support DA release by assessing the impact of
285 isradipine on 1p-evoked $[DA]_o$ in the presence of D2R inhibition. In DLS, isradipine decreased DA release
286 similarly by ~25% in the presence and absence of D2R inhibitor L-741,626 (**Figure 4A,B,** comparison of
287 peaks 1 sample t-test control t_3=6.48 *P*=0.0074; L-741 t_4=4.87 *P*=0.0082). However in NAc, D2R inhibition
288 unsilenced a role for LTCCs in supporting DA release: it enabled an inhibition of $[DA]_o$ by subsequent
289 application of isradipine (**Figure 4C,D,** comparison of peaks 1 sample t-test control: t_3=1.78, *P*=0.19; L-
290 741: t_3=27.56 *P*=0.0001), indicating that D2R activity is limiting LTCC function in NAc but not DLS (**Figure**
291 **4E,** 2-way ANOVA region X L-741: $F_{1,14}$=8.13, *P=0.013,* main effect of region: $F_{1,14}$=16.8, *P*=0.001, main
292 effect of L-741 $F_{1,14}$=14.5 *P*=0.002).

293 Given this apparent role for D2Rs in limiting LTCC support of DA release in NAc, we tested a
294 hypothesis that the mechanism through which cocaine limits LTCC function in DLS might be elevation of

295 DA levels leading to a enhancement of D2R-activation. We inhibited D2Rs with L-741,626, to see if this
296 allowed isradipine to decrease evoked $[DA]_o$ in the presence of cocaine. However, isradipine did not
297 decrease DA release in DLS in the presence of cocaine and L-741,626, indicating that the control of LTCC
298 support of DA release by DATs in DLS is independent of D2R regulation (**Figure 4F,** t-test t_7=1.65 P=0.14).

299 We tested finally whether D2Rs or DATs interact with the effects of Calb1 in NAc on LTCC support
300 of DA release. In NAc of CalbKD mice where LTCCs support DA release (see Fig 2), D2R-inhibition did not
301 augment the impact of isradipine on DA release compared to without D2R inhibition (**Figure 4G-I,**
302 Dunnets post-test t_9=0.3 *P*=0.94) indicating either that the impact of CalbKD and D2R inhibition of LTCC
303 role has reached a ceiling, or that the mechanism through which D2Rs are governing LTCC impact involves
304 Calb1. The inhibition of DATs in NAc of CalbKD mice with cocaine occluded the effect of isradipine on DA
305 release (**Figure 4G-I,** t_2=0.73 *P=0.*53). These data indicate that LTCC support of DA release in NAc in CalbKD
306 mice can be facilitated by DATs (**Figure 4I,** 1-way ANOVA Sidak post-test CalbKD vs cocaine t_9=3.9 *P=0.007*
307 CalbKD vs L471 t_9=0.3 *p=0.94*). These features of DAT support but no D2R control of LTCC function in NAc
308 in CalbKD mice mirror the regulation of LTCC function in DLS of wild-type mice. Together, they also reveal
309 that while Calb1 and D2Rs each limit LTCC function in wild-type NAc they do not do so in DLS (in the
310 presence of normal DAT function).

311 Here, we have shown that the apparent function of LTCCs in supporting DA release varies with a
312 large range of biological conditions, some of which show apparent co-dependencies. To better
313 understand how these factors, of genotype, sex, region and molecular regulators interact to govern
314 whether LTCCs support DA release, and by extension set the conditions when isradipine will decrease DA
315 release, we employed a classification tree algorithm with Gini impurity, for each experimental replicate,
316 to understand the relative influence of each factor (**Figure 5A**). The classification tree illustrated that DAT
317 activity (*cocaine data*) is a key means of supporting L-function; the presence of cocaine is a robust limiter
318 of isradipine's effect. Conversely, *Calb1* and *Gba* strongly limit LTCC function; knockdown of either
319 promoted isradipine action. In contrast, in wild-type, *SNCA*-OVX and *Snca*-null mice, LTCC function co-
320 varied with sex, striatal region, D2-receptor state or cholesterol level (**Figure 5A**). The branching of the
321 tree into multiple pure leaves (each end node had probability of 0 or 1, no outliers) facilitated a
322 straightforward classification of factors into either facilitators or inhibitors of LTCC function (**Figure 5B**).

323 Discussion

324 We reveal here that LTCC support of DA release from DA axons is regulated by multiple, endogenous
325 factors in a regionally and sexually divergent manner. In DLS, LTCCs operate more evidently in males, and
326 their support of DA release is facilitated by α-synuclein and DATs and permitted by the absence of Calb1.
327 In NAc, LTCC support of DA release is prevented by Calb1 and D2Rs. Intriguingly, regulators that promote

328 LTCC function are associated with increased risk of degeneration in PD, while some of those that limit
329 function are associated with reduced neuronal vulnerability, suggesting that intersecting mechanisms
330 regulating DA handing and LTCC function might together contribute to the metabolic load of vulnerable
331 neurons.

332 **Sex differences interact with multiple factors to govern LTCC function**

333 LTCCs have been suggested to confer vulnerability to degeneration of SNc DA neurons in PD (Surmeier,
334 2018), a disease with a higher incidence in men than women (Wooten et al., 2004). Yet, the relative roles
335 of LTCCs in DA neurons in males versus females has been unknown. We reveal there is a greater role for
336 LTCCs in supporting DA release in male DLS than in female, and this raises the speculation that differential
337 LTCC function might contribute to the greater incidence of PD in men than women. Future studies should
338 assess function in both sexes if we are to better understand how to exploit Ca^{2+} biology for a
339 neuroprotective strategy.

340 Alpha-synuclein is well known to be a contributing factor in PD, however its precise physiological
341 and pathological functions remain incompletely characterised (Alegre-Abarrategui et al., 2019). Here we
342 identify in male mice that axonal LTCC support of DA release is dependent on α-synuclein. It should be
343 noted that some commercially available wild-type mouse strains including the Harlan C57Bl6/6S are null
344 for α-synuclein due to a spontaneous deletion (Specht and Schoepfer, 2001), which likely limits LTCC
345 function in that strain also. The mechanism is yet to be determined, but we note a cascade of potentially
346 interacting factors: we previously found that α-synuclein impacts on brain cholesterols and other lipids
347 that shape DAT activity (Threlfell et al., 2021), and found here that cholesterol reinstates an LTCC function
348 lost after α-synuclein deletion in a DAT-dependent manner. Mutations in the *GBA* gene are the most
349 common genetic factors in PD (Smith and Schapira, 2022) and appear especially important in female
350 patients with PD (Li et al., 2021). Here, we show that *GBA* knockdown led to isradipine decreasing DA
351 release in the DLS of *Gba*$^{+/-}$ female mice, indicating that intact GCase activity normally limits how LTCCs
352 support DA release in female mice.

353 The fast Ca^{2+} buffer calbindin-D28k (Calb1) has been considered previously as potentially
354 neuroprotective, but evidence for a neuroprotective role has not mixed. It remains possible that the toxin
355 models typically used are too aggressive to reveal neuroprotection (Airaksinen et al., 1997; Yuan et al.,
356 2013). In any event, we found that Calb1 was important for both regional and sex differences in LTCC
357 regulation of DA release. Under our standard experimental conditions, LTCCs do not contribute to DA
358 release in male NAc (Brimblecombe et al., 2015), and we show here that Calb1 plays a key limiting role.
359 We found also that Calb1 prevents LTCCs from supporting DA release in DLS of females, despite finding
360 previously that Calb1 does not limit the levels of DA released (Brimblecombe et al., 2019). The
361 mechanisms by which Calb1 limits how LTCCs support DA release have not been fully elucidated and are

362 likely to depend on a number of factors, due to the global signalling nature of Ca^{2+} and the ability of Calb1
363 to act as a sink and a source for Ca^{2+} (Schwaller et al., 2002; Schwaller, 2020). Potential mechanisms
364 include: Calb1 buffering Ca^{2+} after entry via LTCCs; Calb1 acting as a Ca^{2+} shuttle to facilitate Ca^{2+}-
365 dependent inactivation (CDI) of LTCC (Lee et al., 2006); or Calb1 reducing activation of LTCC via inhibition
366 of DAT function (see below). The mechanisms through which Calb1 and LTCC interact in a sex-specific
367 manner are also likely to be complex. Sexual dimorphism in LTCC function has been documented in
368 cardiac tissue (Curl et al., 2008; Prabhavathi et al., 2014; Machuki et al., 2019) whilst in the brain, Calb1
369 function can be regulated by sex-linked genes and hormones at transcriptional and protein level (Abel
370 and Rissman, 2012). The mechanisms operating in DA neurons are not yet known but could have
371 important clinical implications for sex-specific incidence of disease and responsiveness to medication.

372 **DAT promotes and D2R limits LTCC support of DA release**

373 We found that LTCC function is supported by DATs, in males in DLS in wild-types and in NAc after calb1
374 knockdown. Correspondingly, electrogenic monoamine transporters including the DAT are documented
375 to promote Ca^{2+} entry via LTCCs in expression systems (Cameron et al., 2015). We speculate that a similar
376 electrogenic mechanism is responsible in DA axons. It is intriguing to note that in NAc, DA uptake rates
377 are greater after calb1 knockdown than in controls (Brimblecombe et al., 2019), supporting a hypothesis
378 that LTCC support of DA release in NAc after Calb1 knockdown might result from the associated impact
379 of elevated DAT on depolarisation, in addition to a more simple explanation that there is reduced Ca^{2+}
380 buffering. The greater LTCC function in DLS than NAc (Brimblecombe et al., 2015) parallels the higher DAT
381 levels in source DA neurons in SNc than VTA (Poulin et al., 2014). However, DAT function alone is not the
382 sole predictor of LTCC function, as LTCC support of DA release in DLS was not different between wild-
383 type and DAT-$Cre^{+/-}$ mice (CalbWT), despite DAT-$Cre^{+/-}$ mice having lower DAT levels and function
384 (Bäckman et al., 2006; Brimblecombe et al., 2019). Alternative explanations for DAT regulation of LTCC
385 function could yet include that LTCCs might regulate DA release in a DAT-dependent manner, so when
386 DAT is inhibited, LTCC dependence is occluded. Our findings together with other literature add to the
387 growing body of evidence that DATs serve more functions than simply clearing extracellular DA, as they
388 participate in the underlying control of DA release (Venton et al., 2006; Kile et al., 2010; Siciliano et al.,
389 2018; Brimblecombe et al., 2019; Condon et al., 2019).

390 We also found that LTCC support of DA release is inhibited by D2Rs, in male NAc. LTCCs have vice
391 versa been shown to regulate D2Rs (Zhang and Sulzer, 2012; Dragicevic et al., 2014; Duda et al., 2016),
392 and therefore together these data show that there is reciprocal regulation between LTCCs and D2Rs.
393 D2Rs have been shown previously to inhibit LTCC function in striatal GABAergic projection neurons, and
394 cultured midbrain neurons (Hernández-López et al., 2000; Yasumoto et al., 2004; Olson et al., 2005) but
395 this effect is somewhat surprising for DA release because D2Rs do not appear to be activated sufficiently

396 in this preparation to be limiting DA release for these stimuli (Kennedy et al., 1992; Cragg, 2003; Condon
397 et al., 2019) suggesting that there is limited tonic activity at D2Rs. An explanation for this disparity could
398 be that for 1p-evoked DA release, there is no net effect of inhibiting D2Rs on $[DA]_o$ due to the wide range
399 of ion channels and intracellular cascades affected by D2Rs, including voltage-gated K^+ channel-
400 dependent mechanisms (Fulton et al., 2011), N- and PQ-type Ca^{2+} channels (Cardozo and Bean, 1995) and
401 LTCC-dependent mechanisms (Hernández-López et al., 2000) (reviewed in (Ford, 2014)). These multiple
402 outcomes of D2R activity might also provide an explanation for why D2Rs were not detected to limit LTCC
403 function in DLS. From these collected observations, it is evident that roles of LTCCs in DA release, and the
404 effects of isradipine, are plastic; they are variable between DA neuron types, they vary with the activity
405 of a range of biological regulatory mechanisms, and experimental conditions, and whether the subjects
406 are males or females.

407 The mechanisms by which LTCCs are supporting DA release, and differently with diverse factors,
408 are not yet resolved. Incoming Ca^{2+} via LTCCs could directly contribute to the Ca^{2+} required for exocytosis
409 or could contribute to other processes that modify DA release probability. Indeed, LTCCs lack the synprint
410 site possessed by several other VGCCs which tethers VGCCs to the exocytotic machinery (Mochida et al.,
411 2003) suggesting LTCCs might not be located in sufficient proximity to catalyse exocytosis directly.
412 Alternatively, LTCCs might support DA release by aiding depolarisation to support AP generation and
413 propagation through the highly branched axonal arbour. They might also couple to Ca^{2+} dependent
414 signalling cascades including those regulated by GPCRs that regulate DA release (Fulton et al., 2011).
415 There is also the possibility that Ca^{2+} entry via LTCCs and downstream activation of RyRs drives
416 mitochondrial generation of ATP (Zampese et al., 2022) that in turn might support axon activity or
417 depolarisation. The factors reported here that change how LTCCs support DA release might change
418 axonal demand for ATP thus driving differing dependencies on Ca^{2+} entry via LTCCs to signal to
419 mitochondria to support the required production of ATP. In turn, since this process contributes a
420 metabolic stress (Pacelli et al., 2015), LTCC function might drive an axonal metabolic stress and also be a
421 reporter for axons with higher metabolic demand. These hypotheses are not mutually exclusive, but are
422 yet to be tested.

423 In summary, we show that the factors that govern the variable role of axonal LTCCs in supporting
424 DA release in DLS versus NAc include α-synuclein, DATs, calb1 and D2Rs. These factors can vary between
425 striatal regions and support LTCC function in DLS whilst preventing LTCC function in NAc, thereby
426 accounting for the disparity between LTCC expression and function in different DA neurons. It is further
427 noteworthy that factors that promote LTCC support of DA release such as male sex, α-synuclein, DAT and
428 the absence of Calb1 correspond to risk factors for parkinsonian degeneration, understanding how these
429 factors interact may allow the stratification of patient cohorts to identify those who would most benefit

430 from targeting LTCC as a neuroprotective strategy with isradipine (Parkinson Study Group STEADY-PD III
431 Investigators, 2020). By facilitating LTCC function these factors might drive metabolic damage to
432 vulnerable neurons, corroborating the hypothesis that LTCCs might then offer a target for a
433 neuroprotective therapy. Alternatively, LTCC support of DA release might be only a readout of
434 vulnerability, a "canary in the coalmine", when in turn, manipulation of LTCC function would not protect
435 vulnerable neurons. The utility of targeting LTCC as a neuroprotective strategy against Parkinson's is likely
436 to depend on there being a net benefit from three competing aspects: firstly, limiting LTCC activity
437 associated with pacemaker function is likely to be beneficial, but only if it outweighs the second factor of
438 reduced dopamine release. Thirdly, it remains to be seen if limiting LTCC associated ATP production is
439 net protective by limiting the production of damaging reactive-oxidative species or damaging, due to it
440 removing a necessary source of ATP. A fuller understanding of the underlying interconnected biology will
441 better inform neuroprotective strategies for PD targeting L-channels and beyond.

References

442 Abel JL, Rissman EF (2012) Location, location, location: Genetic regulation of neural sex differences. Rev
443 Endocr Metab Disord 13:151–161.
444 Acevedo-Rodriguez A, Zhang L, Zhou F, Gong S, Gu H, De Biasi M, Zhou F-M, Dani JA (2014) Cocaine
445 inhibition of nicotinic acetylcholine receptors influences dopamine release. Front Synaptic
446 Neurosci 6:19.
447 Airaksinen MS, Thoenen H, Meyer M (1997) Vulnerability of Midbrain Dopaminergic Neurons in
448 Calbindin-D 28k -deficient Mice: Lack of Evidence for a Neuroprotective Role of Endogenous
449 Calbindin in MPTPtreated and Weaver Mice. Eur J Neurosci 9:120–127.
450 Alegre-Abarrategui J, Brimblecombe KR, Roberts RF, Velentza-Almpani E, Tilley BS, Bengoa-Vergniory N,
451 Proukakis C (2019) Selective vulnerability in α-synucleinopathies. Acta Neuropathol 138:681–704.
452 Bäckman CM, Malik N, Zhang Y, Shan L, Grinberg A, Hoffer BJ, Westphal H, Tomac AC (2006)
453 Characterization of a mouse strain expressing Cre recombinase from the 3' untranslated region of
454 the dopamine transporter locus. Genesis 44:383–390.
455 Barski JJ, Mörl K, Meyer M (2002) Conditional inactivation of the calbindin D-28k (Calb1) gene by
456 Cre/loxP-mediated recombination. Genesis 32:165–168.
457 Bekris LM, Mata IF, Zabetian CP (2010) The genetics of Parkinson disease. J Geriatr Psychiatry Neurol
458 23:228–242.
459 Brimblecombe KR, Gracie CJ, Platt NJ, Cragg SJ (2015) Gating of dopamine transmission by calcium and
460 axonal N, Q, T and L-type voltage-gated calcium channels differs between striatal domains. J
461 Physiol 593:929–946.
462 Brimblecombe KR, Vietti-Michelina S, Platt NJ, Kastli R, Hnieno A, Gracie CJ, Cragg SJ (2019) Calbindin-
463 D28K Limits Dopamine Release in Ventral but Not Dorsal Striatum by Regulating Ca 2+ Availability
464 and Dopamine Transporter Function. ACS Chem Neurosci 10:3419–3426.
465 Cachope R, Mateo Y, Mathur BN, Irving J, Wang H-L, Morales M, Lovinger DM, Cheer JF (2012) Selective
466 activation of cholinergic interneurons enhances accumbal phasic dopamine release: setting the
467 tone for reward processing. Cell Rep 2:33–41.
468 Cameron KN, Solis E, Ruchala I, De Felice LJ, Eltit JM (2015) Amphetamine activates calcium channels
469 through dopamine transporter-mediated depolarization. Cell Calcium 58:457–466.
470 Cardozo DL, Bean BP (1995) Voltage-dependent calcium channels in rat midbrain dopamine neurons:
471 modulation by dopamine and GABAB receptors. J Neurophysiol 74:1137–1148.
472 Ciliax BJ, Heilman C, Demchyshyn LL, Pristupa ZB, Ince E, Hersch SM, Niznik HB, Levey AI (1995) The
473 Dopamine Transporter: lmmunochemical Characterization and Localization in Brain. J Neurosci
474 75:1714–1723.
475 Condon MD, Platt NJ, Zhang YF, Roberts BM, Clements MA, Vietti-Michelina S, Tseu MY, Brimblecombe

476 KR, Threlfell S, Mann EO, Cragg SJ (2019) Plasticity in striatal dopamine release is governed by
477 release-independent depression and the dopamine transporter. Nat Commun 10:1–15.
478 Connor-Robson N, Booth H, Martin JG, Gao B, Li K, Doig N, Vowles J, Browne C, Klinger L, Juhasz P, Klein
479 C, Cowley SA, Bolam P, Hirst W, Wade-Martins R (2019) An integrated transcriptomics and
480 proteomics analysis reveals functional endocytic dysregulation caused by mutations in LRRK2.
481 Neurobiol Dis 127:512–526.
482 Costa KM, Schenkel D, Roeper J (2021) Sex-dependent alterations in behavior, drug responses and
483 dopamine transporter expression in heterozygous DAT-Cre mice. Sci Rep 11:3334.
484 Cragg SJ (2003) Variable Dopamine Release Probability and Short-Term Plasticity between Functional
485 Domains of the Primate Striatum. J Neurosci 23:4378–4385.
486 Curl CL, Delbridge LMD, Wendt IR (2008) Sex differences in cardiac muscle responsiveness to Ca2+ and
487 L-type Ca2+ channel modulation. Eur J Pharmacol 586:288–292.
488 Dragicevic E, Poetschke C, Duda J, Schlaudraff F, Lammel S, Schiemann J, Fauler M, Hetzel A, Watanabe
489 M, Lujan R, Malenka RC, Striessnig J, Liss B (2014) Cav1.3 channels control D2-autoreceptor
490 responses via NCS-1 in substantia nigra dopamine neurons. Brain 137:2287–2302.
491 Duda J, Pötschke C, Liss B (2016) Converging roles of ion channels, calcium, metabolic stress, and
492 activity pattern of *Substantia nigra* dopaminergic neurons in health and Parkinson's disease. J
493 Neurochem 139:156–178.
494 Ford CP (2014) The role of D2-autoreceptors in regulating dopamine neuron activity and transmission.
495 Neuroscience 282:13–22.
496 Fulton S, Thibault D, Mendez JA, Lahaie N, Tirotta E, Borrelli E, Bouvier M, Tempel BL, Trudeau LE (2011)
497 Contribution of Kv1.2 voltage-gated potassium channel to D2 autoreceptor regulation of axonal
498 dopamine overflow. J Biol Chem 286:9360–9372.
499 Gerfen CR, Baimbridge KG, Thibault J (1987) The neostriatal mosaic: III. Biochemical and developmental
500 dissociation of patch-matrix mesostriatal systems. J Neurosci 7:3935–3944.
501 Greene JGJG, Dingledine R, Grenamyre JT, Greenamyre JT (2005) Gene expression profiling of rat
502 midbrain dopamine neurons: implications for selective vulnerability in parkinsonism. Neurobiol Dis
503 18:19–31.
504 Guzman JN, Ilijic E, Yang B, Sanchez-Padilla J, Wokosin D, Galtieri D, Kondapalli J, Schumacker PT,
505 Surmeier DJ (2018) Systemic isradipine treatment diminishes calcium-dependent mitochondrial
506 oxidant stress. J Clin Invest 128:2266–2280.
507 Guzman JN, Sánchez-Padilla J, Chan CS, Surmeier DJ (2009) Robust pacemaking in substantia nigra
508 dopaminergic neurons. J Neurosci 29:11011–11019.
509 Helton TD, Xu W, Lipscombe D (2005) Neuronal L-type calcium channels open quickly and are inhibited
510 slowly. J Neurosci 25:10247–10251.

511 Hernández-López S, Tkatch T, Perez-Garci E, Galarraga E, Bargas J, Hamm H, Surmeier DJ (2000) D2
512 Dopamine Receptors in Striatal Medium Spiny Neurons Reduce L-Type Ca2+ Currents and
513 Excitability via a Novel PLCβ1–IP3–Calcineurin-Signaling Cascade. J Neurosci 20:8987–8995.
514 Ilijic E, Guzman JN, Surmeier DJ (2011) The L-type channel antagonist isradipine is neuroprotective in a
515 mouse model of Parkinson's disease. Neurobiol Dis 43:364–371.
516 Ingram SL, Prasad BM, Amara SG (2002) Dopamine transporter-mediated conductances increase
517 excitability of midbrain dopamine neurons. Nat Neurosci.
518 Janezic S et al. (2013) Deficits in dopaminergic transmission precede neuron loss and dysfunction in a
519 new Parkinson model. Proc Natl Acad Sci U S A 110:E4016-25.
520 Kang S, Cooper G, Dunne SF, Luan C-H, Surmeier DJ, Silverman RB (2013) Structure-activity relationship
521 of N,N'-disubstituted pyrimidinetriones as Ca(V)1.3 calcium channel-selective antagonists for
522 Parkinson's disease. J Med Chem 56:4786–4797.
523 Kennedy RT, Jones SR, Wightman RM (1992) Dynamic Observation of Dopamine Autoreceptor Effects in
524 Rat Striatal Slices. J Neurochem 59:449–455.
525 Kile BM, Guillot TS, Venton BJ, Wetsel WC, Augustine GJ, Wightman RM (2010) Synapsins differentially
526 control dopamine and serotonin release. J Neurosci 30:9762–9770.
527 Lee D, Obukhov AG, Shen Q, Liu Y, Dhawan P, Nowycky MC, Christakos S (2006) Calbindin-D28k
528 decreases L-type calcium channel activity and modulates intracellular calcium homeostasis in
529 response to K+ depolarization in a rat beta cell line RINr1046-38. Cell Calcium 39:475–485.
530 Li Q, Jing Y, Lun P, Liu X, Sun P (2021) Association of gender and age at onset with glucocerebrosidase
531 associated Parkinson's disease: a systematic review and meta-analysis. Neurol Sci 42:2261–2271.
532 Lohr KM, Masoud ST, Salahpour A, Miller GW (2017) Membrane transporters as mediators of synaptic
533 dopamine dynamics: implications for disease. Eur J Neurosci 45:20–33.
534 Machuki JO, Zhang H-Y, Geng J, Fu L, Adzika GK, Wu L, Shang W, Wu J, Kexue L, Zhao Z, Sun H (2019)
535 Estrogen regulation of cardiac cAMP-L-type Ca2+ channel pathway modulates sex differences in
536 basal contraction and responses to β2AR-mediated stress in left ventricular apical myocytes. Cell
537 Commun Signal 17:34.
538 Mochida S, Westenbroek RE, Yokoyama CT, Zhong H, Myers SJ, Scheuer T, Itoh K, Catterall WA (2003)
539 Requirement for the synaptic protein interaction site for reconstitution of synaptic transmission
540 by P/Q-type calcium channels. Proc Natl Acad Sci U S A 100:2819–2824.
541 Olson PA, Tkatch T, Hernandez-Lopez S, Ulrich S, Ilijic E, Mugnaini E, Zhang H, Bezprozvanny I, Surmeier
542 DJ (2005) G-protein-coupled receptor modulation of striatal CaV1.3 L-type Ca2+ channels is
543 dependent on a Shank-binding domain. J Neurosci 25:1050–1062.
544 Pacelli C, Giguère N, Bourque M-J, Lévesque M, Slack RS, Trudeau L-É (2015) Elevated Mitochondrial
545 Bioenergetics and Axonal Arborization Size Are Key Contributors to the Vulnerability of Dopamine

546 Neurons. Curr Biol 25:2349–2360.
547 Parkinson Study Group STEADY-PD III Investigators (2020) Isradipine Versus Placebo in Early Parkinson
548 Disease. Ann Intern Med 172:591–598.
549 Poulin J-F, Zou J, Drouin-Ouellet J, Kim K-YA, Cicchetti F, Awatramani RB (2014) Defining midbrain
550 dopaminergic neuron diversity by single-cell gene expression profiling. Cell Rep 9:930–943.
551 Prabhavathi K, Selvi KT, Poornima KN, Sarvanan A (2014) Role of biological sex in normal cardiac
552 function and in its disease outcome - a review. J Clin Diagn Res 8:BE01-4.
553 Rey S, Maton G, Satake S, Llano I, Kang S, Surmeier DJ, Silverman RB, Collin T (2020) Physiological
554 involvement of presynaptic L-type voltage-dependent calcium channels in GABA release of
555 cerebellar molecular layer interneurons. J Neurochem 155:390–402.
556 Rice ME, Cragg SJ (2004) Nicotine amplifies reward-related dopamine signals in striatum. Nat Neurosci
557 7:583–584.
558 Ritz BR, Manthripragada AD, Costello S, Lincoln SJ, Farrer MJ, Cockburn M, Bronstein J (2009) Dopamine
559 transporter genetic variants and pesticides in Parkinson's disease. Environ Health Perspect
560 117:964–969.
561 Roberts BM, Doig NM, Brimblecombe KR, Lopes EF, Siddorn RE, Threlfell S, Connor-Robson N, Bengoa-
562 Vergniory N, Pasternack N, Wade-Martins R, Magill PJ, Cragg SJ (2020) GABA uptake transporters
563 support dopamine release in dorsal striatum with maladaptive downregulation in a parkinsonism
564 model. Nat Commun 11:4958.
565 Schwaller B (2020) Cytosolic Ca2+ buffers are inherently Ca2+ signal modulators. Cold Spring Harb
566 Perspect Biol 12:a035543.
567 Schwaller B, Meyer M, Schiffmann S (2002) "New" functions for "old" proteins: the role of the calcium-
568 binding proteins calbindin D-28k, calretinin and parvalbumin, in cerebellar physiology. Studies
569 with knockout mice. Cerebellum 1:241–258.
570 Siciliano CA, Saha K, Calipari ES, Fordahl SC, Chen R, Khoshbouei H, Jones SR (2018) Amphetamine
571 Reverses Escalated Cocaine Intake via Restoration of Dopamine Transporter Conformation. J
572 Neurosci 38:484–497.
573 Smith L, Schapira AHV (2022) GBA Variants and Parkinson Disease: Mechanisms and Treatments. Cells
574 11.
575 Sonders MS, Zhu SJ, Zahniser NR, Kavanaugh MP, Amara SG (1997) Multiple ionic conductances of the
576 human dopamine transporter: The actions of dopamine and psychostimulants. J Neurosci.
577 Specht CG, Schoepfer R (2001) Deletion of the alpha-synuclein locus in a subpopulation of C57BL/6J
578 inbred mice. BMC Neurosci 2:11.
579 Surmeier DJ (2018) Determinants of dopaminergic neuron loss in Parkinson's disease. FEBS J 285:3657–
580 3668.

581 Surmeier DJ, Guzman JN, Sanchez-Padilla J (2010) Calcium, cellular aging, and selective neuronal
582 vulnerability in Parkinson's disease. Cell Calcium 47:175–182.
583 Threlfell S, Lalic T, Platt NJ, Jennings KA, Deisseroth K, Cragg SJ (2012) Striatal dopamine release is
584 triggered by synchronized activity in cholinergic interneurons. Neuron 75:58–64.
585 Threlfell S, Mohammadi AS, Ryan BJ, Connor-Robson N, Platt NJ, Anand R, Serres F, Sharp T, Bengoa-
586 Vergniory N, Wade-Martins R, Ewing A, Cragg SJ, Brimblecombe KR (2021) Striatal Dopamine
587 Transporter Function Is Facilitated by Converging Biology of α-Synuclein and Cholesterol. Front
588 Cell Neurosci 15.
589 Venton BJ, Seipel AT, Phillips PEM, Wetsel WC, Gitler D, Greengard P, Augustine GJ, Wightman RM
590 (2006) Cocaine increases dopamine release by mobilization of a synapsin-dependent reserve pool.
591 J Neurosci 26:3206–3209.
592 Wooten GF, Currie LJ, Bovbjerg VE, Lee JK, Patrie J (2004) Are men at greater risk for Parkinson's disease
593 than women? J Neurol Neurosurg Psychiatry 75:637–639.
594 Yasumoto F, Negishi T, Ishii Y, Kyuwa S, Kuroda Y, Yoshikawa Y (2004) Dopamine Receptor 2 Regulates
595 L-Type Voltage-Gated Calcium Channel in Primary Cultured Mouse Midbrain Neural Network. Cell
596 Mol Neurobiol 2004 246 24:877–882.
597 Yuan H-H, Chen R-J, Zhu Y-H, Peng C-L, Zhu X-R (2013) The neuroprotective effect of overexpression of
598 calbindin-D(28k) in an animal model of Parkinson's disease. Mol Neurobiol 47:117–122.
599 Zampese E, Wokosin DL, Gonzalez-Rodriguez P, Guzman JN, Tkatch T, Kondapalli J, Surmeier WC,
600 D'Alessandro KB, De Stefani D, Rizzuto R, Iino M, Molkentin JD, Chandel NS, Schumacker PT,
601 Surmeier DJ (2022) Ca2+ channels couple spiking to mitochondrial metabolism in substantia nigra
602 dopaminergic neurons. Sci Adv 8.
603 Zhang H, Sulzer D (2012) Regulation of striatal dopamine release by presynaptic auto- and
604 heteroreceptors. Basal Ganglia 2:5–13.
605 Zhou FM, Liang Y, Dani JA (2001) Endogenous nicotinic cholinergic activity regulates dopamine release
606 in the striatum. Nat Neurosci 4:1224–1229.
607

FIGURES and LEGENDS

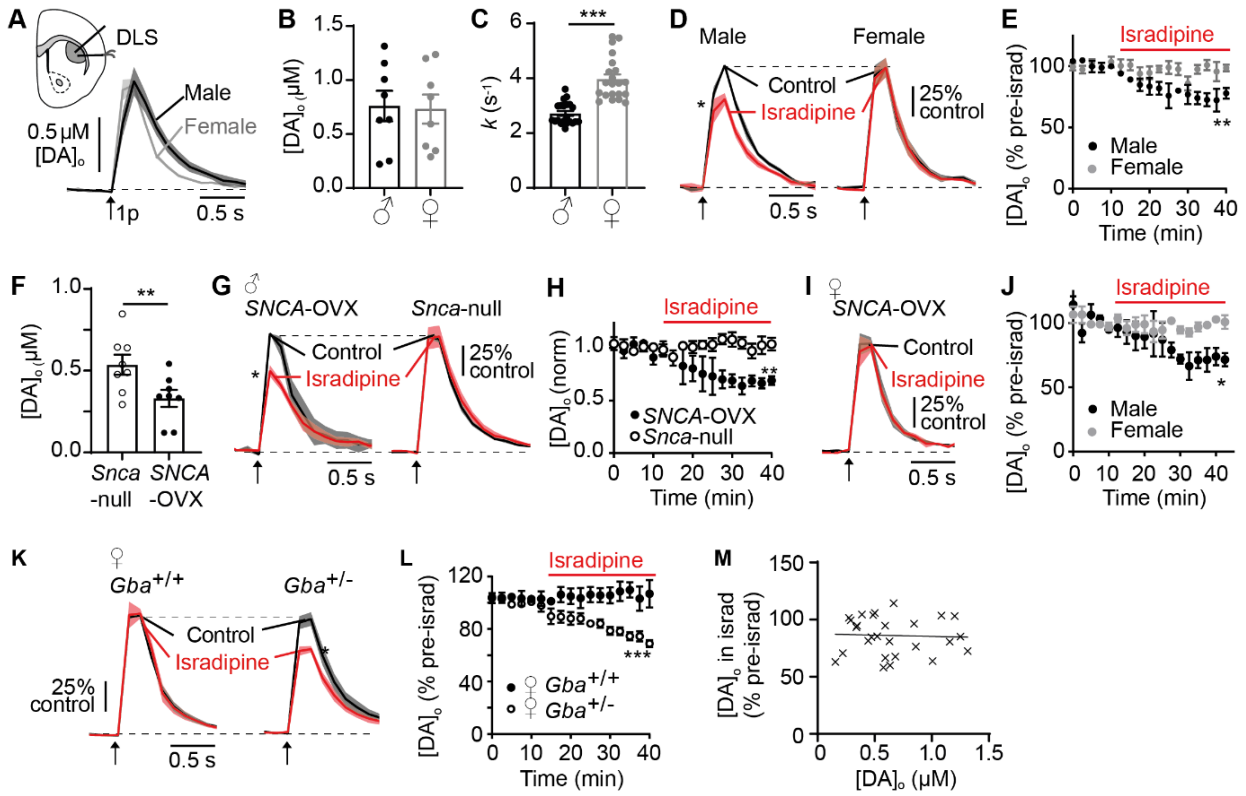

Figure 1. Male sex, presence of α-synuclein, and knockdown of GBA promote LTCC support of DA release in DLS. (**A**) Mean $[DA]_o$ ± SEM vs time evoked by a single pulse (1p, *arrow*) in DLS of male (*black*) versus female (*grey*) wild-type mice. (**B**) Summary of peak evoked $[DA]_o$ ± SEM, N = 6 mice. (**C**) Decay constants of falling phases of 1p-evoked DA transients in DLS of male versus female wild-type mice. Data from N = 12 transients from 6 mice. (**D**) Mean transients for $[DA]_o$ ± SEM vs time evoked by 1p (*arrow*) in control conditions (*black*) versus isradipine (5 µM, *red*) in male (*left*) and female (*right*) normalised to own control. (**E**) Peak $[DA]_o$ ± SEM as % of pre-isradipine control levels versus time. N = 3 male, 5 female. (**F**) Summary of peak $[DA]_o$ evoked by 1p in DLS from male *SNCA*-OVX vs *Snca*-null mice. N = 8 mice. (**G**) Mean $[DA]_o$ ± SEM vs time evoked by 1p (*arrow*) in control versus isradipine in *SNCA*-OVX (*left*) and *Snca*-null (*right*), normalised to control. (**H**) Peak $[DA]_o$ ± SEM as % of pre-isradipine control levels vs time. N= 4 mice. (**I**) Mean $[DA]_o$ ± SEM vs time evoked by 1p (*arrow*) in control and isradipine in female SNCA-OVX mice, normalised to control. N = 3 mice. (**J**) Peak $[DA]_o$ ± SEM as % of pre-isradipine control levels vs time of female vs male *SNCA*-OVX mice. (**K**) Mean $[DA]_o$ ± SEM vs time evoked by 1p (*arrow*) in DLS in control and isradipine in female wild-type ($Gba^{+/+}$) versus GBA-het ($Gba^{+/-}$) mice, normalised to control. (**L**) Peak $[DA]_o$ ± SEM as % of pre-isradipine control levels vs time for female $Gba^{+/+}$ (N=3) versus $Gba^{+/-}$ mice (N=5). (**M**) Peak $[DA]_o$ in isradipine (as % of pre-isradipine control levels) versus peak $[DA]_o$ (µM) in pre-isradipine control conditions plotted for all data shown in conditions in A-L. *< 0.05 ** <0.01 ***<0.001.

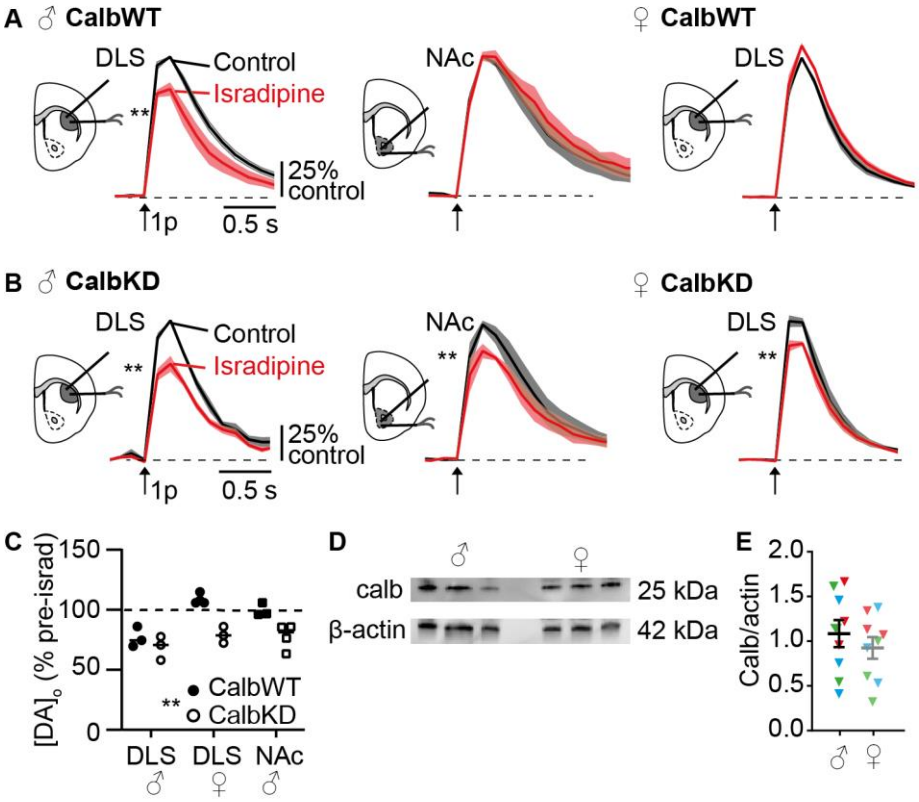

Figure 2. Calb1 limits LTCC function in NAc in male mice, and in DLS in female mice. (**A,B**) Mean $[DA]_o$ ± SEM vs time evoked by single pulses (1p, *arrow*) in control and isradipine (5 µM, *red*) in (A) CalbWT mice or (B) CalbKD mice, in male DLS (*left*), male NAc (*centre*), and female DLS (*right*) normalised to their own control conditions. ** *P*<0.01 comparison of peak $[DA]_o$(**C**) Summary of peak $[DA]_o$ remaining after isradipine (% of pre-isradipine control) in CalbWT and CalbKD striatum. ** *P*<0.01 Effect of genotype 2-way ANOVA. N= 3 pairs DLS male and female N=4 NAc (**D**) Representative examples of Western blots for 3 male and 3 female showing actin (42 kDa) and Calb1 (25 kDa). (**E**) Calbindin-D28K/β-actin protein ratios in male and female striatum. Mean ± SEM; colours group technical replicates (i.e blue points correspond to blot shown in C, and are samples from which stats correspond to, N=3 brains, repeated for 3 blots, illustrated by red, green and blue)

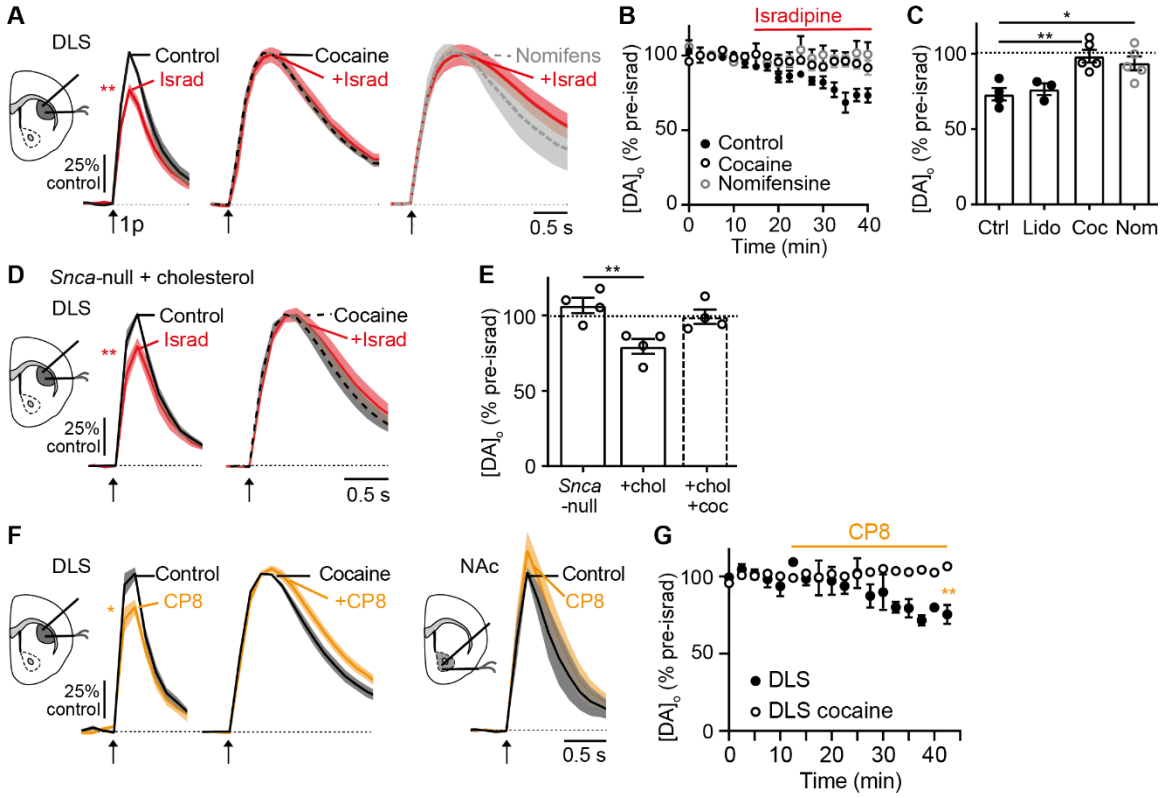

Figure 3. LTCC support of DA release is facilitated by DATs. (**A**) Mean $[DA]_o$ ± SEM vs time evoked by single pulses (1p, *arrow*) in male mice in DLS in control versus isradipine (5 µM, *red*) alone (*left*), or in the presence of cocaine (*centre*), or nomifensine (*right*). (**B**) Peak $[DA]_o$ ± SEM (normalised to pre-isradipine level) vs time in control (*black*), cocaine (unfilled) or nomifensine (grey unfilled). (**C**) Summary of peak $[DA]_o$ remaining after isradipine (% of pre-isradipine control) in DLS of male mice in control (Ctrl) N= 3, lidocaine (*Lido*) N= 3, cocaine (*Coc*) N= 5 or nomifensine (*Nom*) N= 5. (**D**) Mean $[DA]_o$ ± SEM vs time evoked by 1p (*arrow*) in DLS in control versus isradipine in *SNCA*-null tissue incubated in cholesterol (*left*) versus cocaine (*right*). (**E**) Summary of peak $[DA]_o$ remaining after isradipine (% of pre-isradipine control) in DLS of male *Snca*-null mice in control N= 4, cholesterol incubation N= 4, or cholesterol incubation + cocaine. N= 4 (**F**) Mean $[DA]_o$ ± SEM vs time evoked by 1p (*arrow*) in control and CP8 (10 µM, *yellow*) in DLS in control conditions (*left*), in DLS in the prior presence of cocaine (*centre*), or in NAc in control conditions (*right*). (**G**) Peak $[DA]_o$ ± SEM (normalised to pre-CP8 level) vs time in DLS in control (*black*) versus cocaine (unfilled), N=4. *P<0.05 ** P<0.01

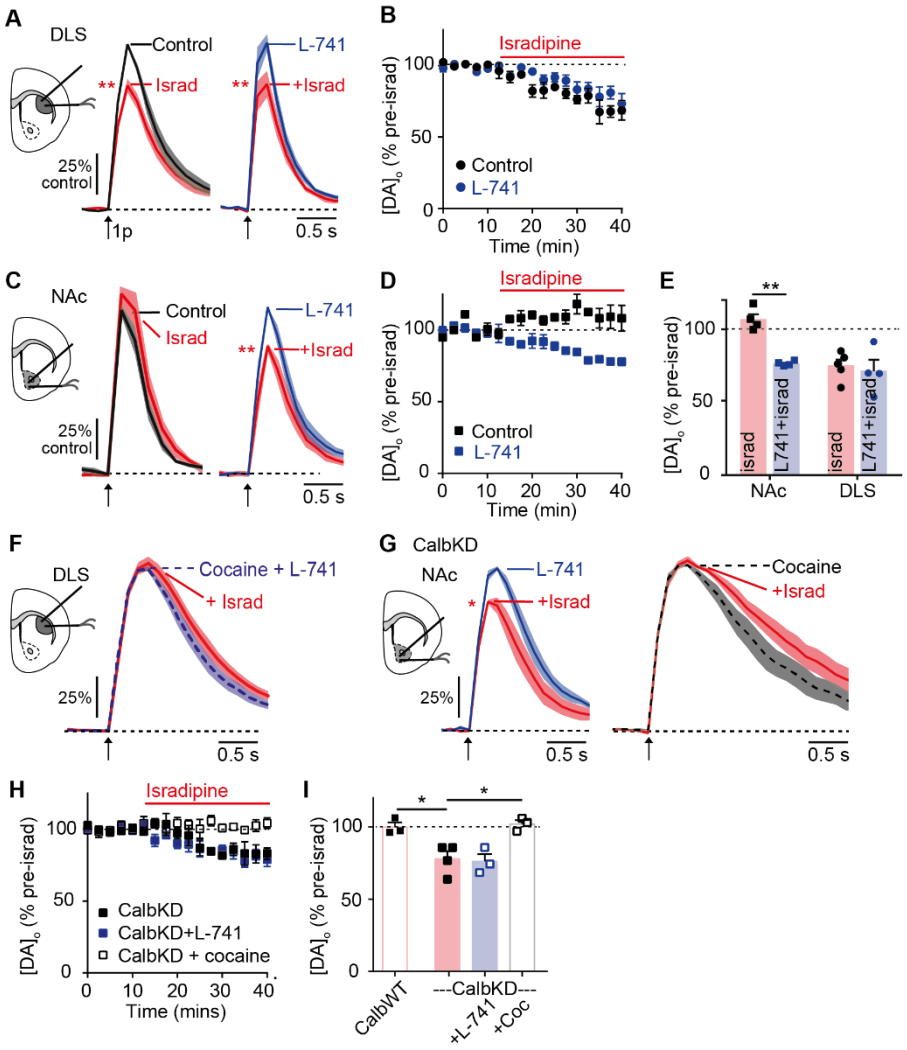

Figure 4. LTCC support of DA release is silenced by D2R. (**A,C**) Mean $[DA]_o$ ± SEM vs time evoked by single pulses (1p, *arrow*) in wild-type male mice in DLS (A) or NAc (C) in control versus isradipine (5 µM, *red*) alone (*left*) or in the presence of D2R-antagonist L-741,626 (2 µM, *right*). (**B,D**) Peak $[DA]_o$ ± SEM (normalised to pre-isradipine level) vs time in control (*black*) or L-741,626 (*blue*) in DLS (B) or NAc (D). (**E**) Summary of peak $[DA]_o$ remaining after isradipine (% of pre-isradipine control), In NAc and CPu without (red) or with L-741 (blue) (N=4) (**F**) Mean $[DA]_o$ ± SEM vs time evoked by 1p (*arrow*) in DLS in the presence of cocaine + L-741,626 (*blue dashed*) alone, or with isradipine (*red*). (**G**) Mean $[DA]_o$ ± SEM vs time evoked by 1p (*arrow*) in NAc from CalbKD mice with and without isradipine in the prior presence of either L-741,626 (*left*), or cocaine (*right*). (**H**) Peak $[DA]_o$ ± SEM (% of pre-isradipine level) vs time during isradipine application in NAc from CalbKD mice in control conditions (*black*), or the presence of L-741,626 (*blue*), or cocaine (*unfilled*). (**I**) Summary of peak $[DA]_o$ remaining after isradipine (% of pre-isradipine control) in NAc in CalbWT (N = 3)or CalbKD mice, N=4 with L-741 (N= 3) or cocaine (N= 3). * $P<0.05$ ** $P<0.01$

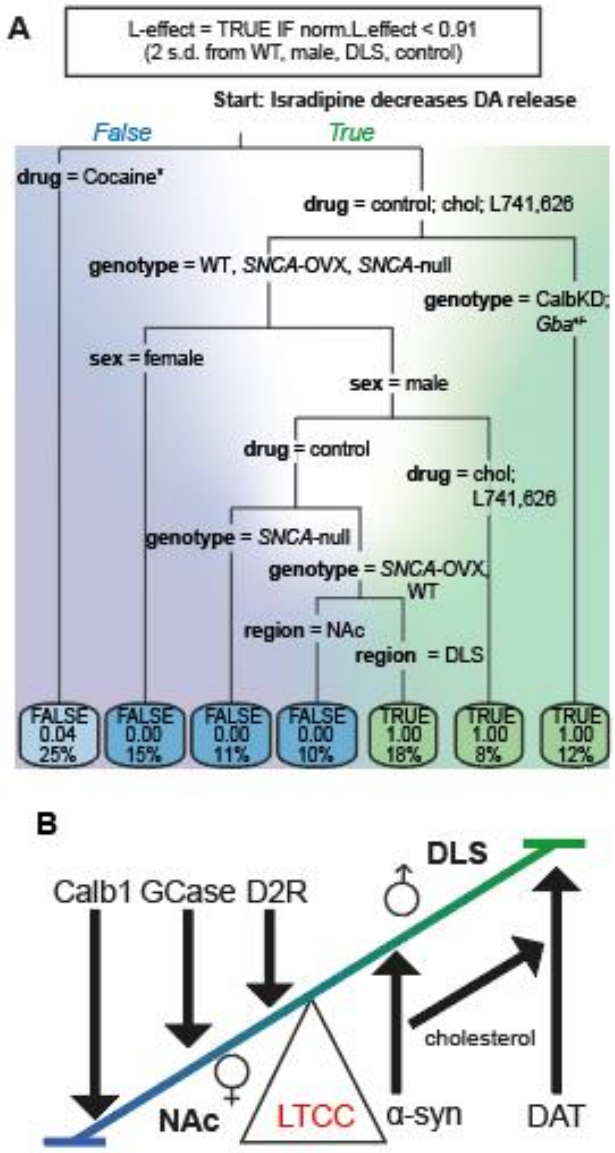

Figure 5: Segregation of factors to facilitators or attenuators of LTCC support of DA release. (**A**) Decision tree segregating experimental conditions of sex, genotype and drug condition using the Gini index. Blue to green background shading shows predictive power of a FALSE (blue) or TRUE (green) outcome respectively. White area shows high uncertainty. Labels on branches indicate recording condition. Left branches for "isradipine decreases DA release" are FALSE. Labels on final boxes (leaves) indicate outcome: TRUE/FALSE (*top*), probability of outcome being correct i.e. 0 or 1 indicate all data from that branch has been correctly sorted (*middle*) and % of datapoints contained within each leaf (*bottom*). *Cocaine is the presence of cholesterol or L-741,626. (**B**) Cartoon illustrating which endogenous factors limit (downward arrows) or promote (upward arrows) LTCC support of DA release.